

Expression of intercellular junctions during preimplantation development of the human embryo

Kate Hardy¹, Anne Warner², Robert M.L. Winston¹ and David L. Becker^{2,3}

¹Human Embryology Laboratory, Institute of Obstetrics and Gynaecology, Royal Postgraduate Medical School, Hammersmith Hospital, Du Cane Road, London W12 0NN, and ²Department of Anatomy and Developmental Biology, University College London, Gower Street, London WC1E 6BT, UK

³To whom correspondence should be addressed

A total of 74 human embryos were stained with gap junction protein specific anti-peptide antibodies and antibodies to the desmosomal protein desmoplakin to reveal the expression pattern of intercellular junctions during preimplantation development. Prior to implantation, the human embryo expresses predominantly connexin (Cx43)-containing gap junctions. Gap junctions were first detected in apposing cell membranes at the 4-cell stage and became increasingly organized as development proceeded. In normal blastocysts, trophoblast (TE) cells were linked by dense arrays of gap junctions while inner cell mass (ICM) cells were linked by small, punctate gap junctions. Gap junctions containing Cx32 or Cx26 were observed occasionally in the TE of late blastocysts. Desmosomes appeared between outer cells prior to cavitation and were retained in the TE, but not in the ICM. Levels of gap junction protein expression were variable in morphologically normal embryos at the same stage, suggesting that a normal appearance may not be a reliable indicator of future viability. Morphologically normal embryos often possessed multinucleate, apoptotic and decompacting cells. They could show either extensive, disorganized over-expression or reduced expression of gap junction protein. The results fit the view that only embryos destined to survive display an organized pattern of intercellular junctions.

Key words: blastocyst/connexin/desmosome/gap junction/immunocytochemistry

Introduction

Pregnancy rates following in-vitro fertilization (IVF) and subsequent embryo transfer are low, averaging only 17% per cycle in the UK in 1992 (Human Fertilisation and Embryology Authority, 1994). In-vitro studies suggest that a large proportion of embryonic loss occurs during preimplantation stages (Hardy, 1993). While 95% of human zygotes successfully undergo the first two cleavage divisions following IVF, ~60% of preimplantation embryonic arrest *in vitro* after the 8-cell stage, at the time of compaction and blastocyst formation.

In the preimplantation mouse embryo, it has been demonstrated that good gap junctional communication is essential for the maintenance of compaction and subsequent preimplantation development (Buehr *et al.*, 1987; Lee *et al.*, 1987; Bevilacqua *et al.*, 1989; Becker *et al.*, 1995). In the early embryos of all species so far examined cells are linked by gap junctions, intercellular structures that allow the transfer of ions and small molecules directly from one cell to the next (for review, see Warner, 1992). The cells of the early mouse embryo are linked by morphologically recognizable gap junctions from the 8-cell stage onwards, when the embryo begins to compact (Ducibella *et al.*, 1975) and from this time onwards all cells exchange low molecular weight dyes, such as Lucifer Yellow, efficiently (Lo and Gilula, 1979). Dye transfer, which indicates the presence of communicating gap junctions, persists between all cells to the late blastocyst stage. The proteins that make up these gap junctions can be recognized by immunocytochemical

staining of the constituent gap junction (connexin) proteins from the 8-cell stage onwards.

Here, using immunocytochemical techniques coupled with confocal microscopy, we have compared gap junction expression in preimplantation human embryos with that found in the early mouse embryo. We report the time course of appearance and the distribution of gap junctions in early human embryos, detected with anti-peptide antibodies specific for three of the connexin proteins that make up gap junctions. We also have examined the appearance of one of the major desmosomal proteins, desmoplakin.

The work was approved by the research ethics committee of the Royal Postgraduate Medical School, Hammersmith Hospital and licensed by the Human Fertilisation and Embryology Authority.

Materials and methods

Ovarian stimulation, oocyte retrieval and embryo culture

Patients had pituitary desensitization with a luteinizing hormone-releasing hormone agonist (LHRH, buserelin; Hoechst, Hounslow, UK). Ovarian stimulation was started with human menopausal gonadotrophin (HMG; Pergonal, Serono, Welwyn Garden City, UK) once oestradiol concentrations were <100 pmoles/l. When 3 or more follicles were at least 17 mm in diameter and serum oestradiol concentrations were >3500 pmoles/l, 10 000 IU human chorionic gonadotrophin (HCG; Profasi, Serono) was given. Oocyte retrieval took place 34–36 h later.

Table I. Labelling of gap junctions, desmosomes and tight junctions in human embryos between day 2 and day 7 post-insemination

Stage	PN ^a	Age ^b	n	Primary antibody					
				Cx43	Cx26	Cx32	DP121	ZO1	None ^c
4-cell	2	2 ^d	5	5	–	–	–	–	–
	< > 2	2 ^d	2	1	–	–	–	–	1
5- to 7-cell	2	2–3 ^e	8	8	–	–	–	1 ^g	–
	< > 2	4	1	1	–	–	–	–	–
8-cell	2	3–4 ^f	9	9	–	–	1 ^h	–	1
	< > 2	3–4	9	9	–	–	1 ^h	–	–
9–16-cell	2	3–4	13	13	–	–	6 ^h	2 ^g	1
Morula	2	4–5	3	3	–	–	1 ^h	–	–
Blastocyst	2	5–7	24	14	7 ⁱ	6	3 ^j	3 ^j	1

^aNumber of pronuclei (PN) visible on day 1: 2 = normally fertilized embryos; < > 2 = parthenogenetic or polyspermic embryos respectively.

^bAge of embryos in days after insemination (day 0).

^cControl embryos with no primary antibody labelling, but with secondary antibody.

^dOne embryo was an arrested day 3 embryo.

^eOne embryo was an arrested day 4 embryo.

^fTwo embryos were arrested day 5 embryos.

^gSimultaneously labelled with ZO1 and Cx43 primary antibodies.

^hSimultaneously labelled with DP121 and Cx43 primary antibodies.

ⁱSimultaneously labelled with Cx26 and Cx43 primary antibodies.

^jSimultaneously labelled with DP121 and ZO1 primary antibodies.

Preincubation, insemination of oocytes and embryo culture were carried out in Earle’s balanced salt solution (EBSS; Gibco BRL, Paisley, UK) supplemented with 25 mM sodium bicarbonate (BDH, Lutterworth, UK), 0.47 mM pyruvic acid (Sigma, Poole, UK) and 10% (v/v) heat-inactivated patient’s serum under a gas phase of 5% CO₂, 5% O₂ and 90% N₂ (Dawson *et al.*, 1995). When the patient’s own serum was not available, human serum albumin (HSA; Zenalab 20, BPL, Elstree, UK) was used at 2.5% (v/v). Individual oocyte–cumulus complexes were inseminated (day 0) 4–6 h after retrieval.

Classification and grading of embryos

Oocytes and embryos were classified according to the number of pronuclei visible on day 1 (16 h after insemination) as: (i) normally fertilized embryos (with two pronuclei); (ii) polyspermic embryos (with three or more pronuclei); and (iii) unfertilized oocytes (with one or no pronucleus). Unfertilized oocytes that subsequently cleaved were classified as parthenogenetic embryos. Following assessment of the number of pronuclei, oocytes and embryos were placed individually in fresh tubes of EBSS containing 10% maternal serum and cultured for a further 24 or 48 h.

On the morning of embryo transfer (either day 2 or 3), embryos were examined and the number of cells determined. Each embryo was then graded according to Dawson *et al.* (1995): grade 1 = perfectly symmetrical with no fragmentation; grade 2 = uneven blastomeres and/or slight fragmentation; grade 3 = uneven with one blastomere fragmented; grade 4 = only one intact blastomere with gross fragmentation; grade 5 = totally degenerate. Embryos of the best morphology and at the most advanced stage of development were selected for transfer.

After confirming the patients’ consent, surplus embryos were allowed to continue development *in vitro* in the original 1 ml of medium, and collected at intervals for immunocytochemistry.

Immunocytochemistry

All embryos were examined using an inverted light microscope with ×20 or ×40 objectives and photographed under interference contrast optics with an Olympus OM2 camera and Ektachrome Elite 400 ASA film to provide a record of individual embryo morphology and developmental stage. Embryos were processed individually so that

light microscope morphology and the pattern of immunostaining could be compared. Appropriate combinations of rabbit and mouse primary antibodies with fluorescein isothiocyanate (FITC) anti-rabbit or (CY5) anti-mouse secondary antibodies allowed two junctional proteins to be labelled simultaneously. Washing and diluting solutions [phosphate-buffered saline (PBS) ‘A’ Oxoid, Basingstoke, UK] were filtered with a 0.22 µm Millipore filter; antibody-containing solutions were centrifuged briefly immediately prior to use.

After photography, embryos were transferred to glass cavity blocks, washed in PBS to remove serum, briefly (2 min) fixed in methanol, and incubated for 45 min in 0.1 M lysine (Sigma) in PBS containing 0.1% Triton X-100 (Sigma). After two washes in PBS each identified embryo was transferred into a 10 µl drop of PBS containing antibodies overlaid with silicone fluid (200/50 cs, BDH, Poole, UK) in a 60 mm petri dish and incubated either for 1 h at 37°C (1:10 antibody dilution in PBS) or overnight at room temperature (1:100 antibody dilution in PBS) in one or more of the following primary antibodies: (i) HJ/gap15, a rabbit polyclonal anti-peptide antibody to the cytoplasmic loop region of connexin 43 (characterized in Becker *et al.*, 1995); (ii) a commercial mouse monoclonal antibody against a sequence from the carboxy tail of connexin 43 (Zymed, San Francisco, CA, USA); (iii) Des5, a rabbit polyclonal anti-peptide antibody to the cytoplasmic loop region of connexin 32; (iv) Des3, a rabbit polyclonal anti-peptide antibody to the cytoplasmic loop region of connexin 26 (see Becker *et al.*, 1995); (v) DP121, a rabbit polyclonal anti-peptide antibody to desmoplakin; and (vi) ZO1, a monoclonal antibody against the ZO1 (kindly donated by Bruce Stevenson) component of tight junctions. The use of two antibodies, raised in different species and against different epitopes of connexin 43 firstly allowed the simultaneous labelling of two different junctional proteins and secondly confirmed that the staining patterns of connexin 43 were not artefacts. After brief washes in PBS, embryos were transferred to 10 µl PBS drops containing FITC labelled swine-anti-rabbit secondary antibodies (DAKO, Copenhagen, Denmark) (1:20) and/or CY5-labelled goat-anti-mouse secondary antibodies (Cambridge Bioscience, Cambridge UK) (1:100) and incubated for 1 h at 37°C. Exposure to light was minimized during and following secondary antibody incubation. Embryos were then washed twice (10 min) in PBS. In later experiments, the first wash contained 1 µg/ml propidium

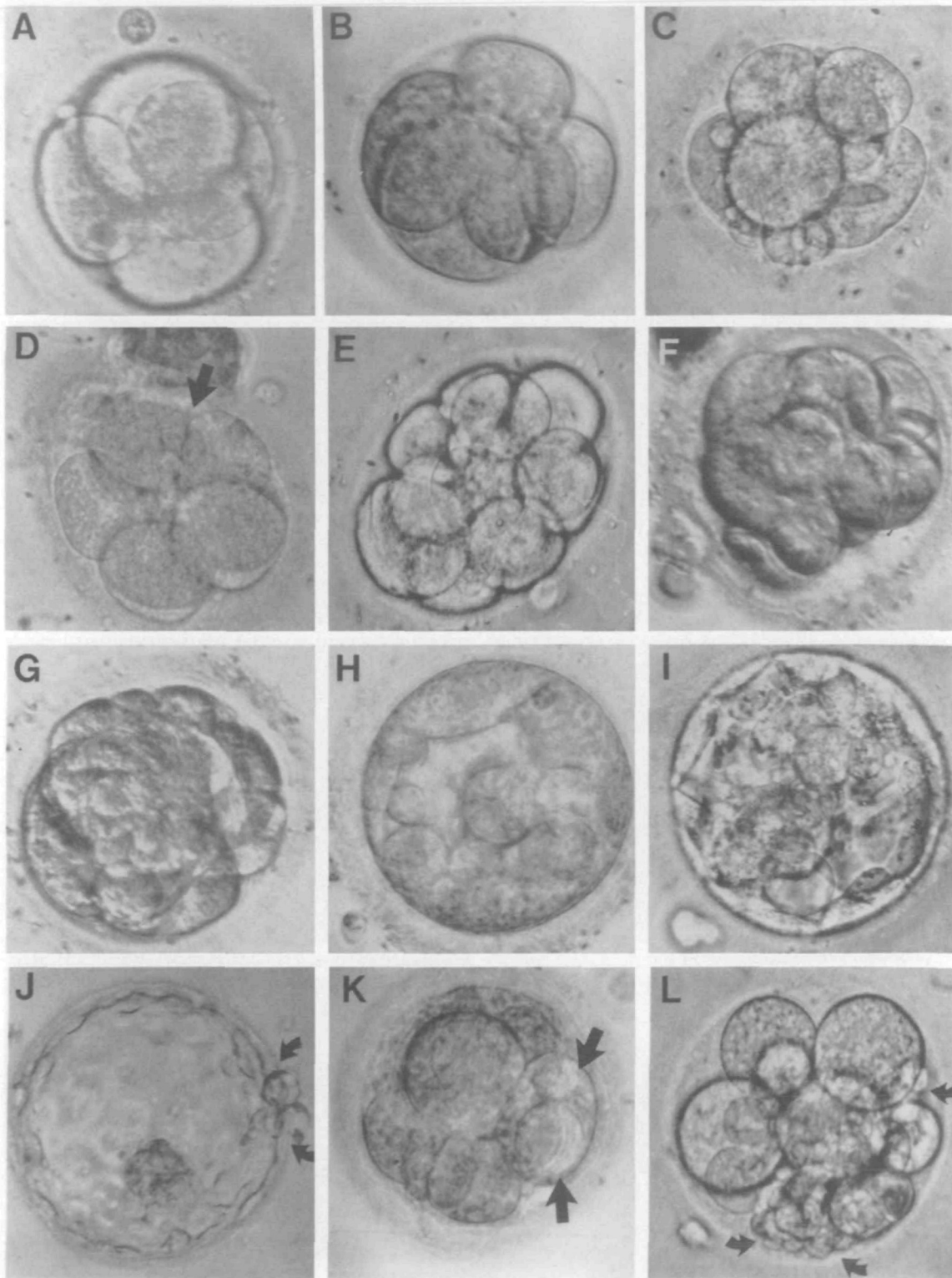


Figure 1. Phase contrast micrographs of normally fertilized human embryos on days 2–6 after insemination (day 0). (A) 4-cell on day 2; (B) 5-cell on day 2; (C) 6-cell on day 3; (D) 8-cell on day 3 with some flattening (arrowed) between blastomeres; (E) 14-cell on day 3 showing absence of compaction; (F) day 4 embryo at ~12-cell stage showing compaction between blastomeres; (G) cavitating morula on day 4 showing poor compaction; (H) early blastocyst on day 5. Note the round, large inner cell mass (ICM) cells with limited attachment to each other; (I) day 5 expanding blastocyst with diffuse ICM consisting of round cells; (J) expanded blastocyst on day 6 with compacted, discrete ICM. The blastocyst is starting to herniate (arrowed); (K) arrested 8-cell embryo on day 5. Note the vacuolated blastomere (arrowed); (L) day 3 embryo with ~6 cells showing fragmentation (arrowed).

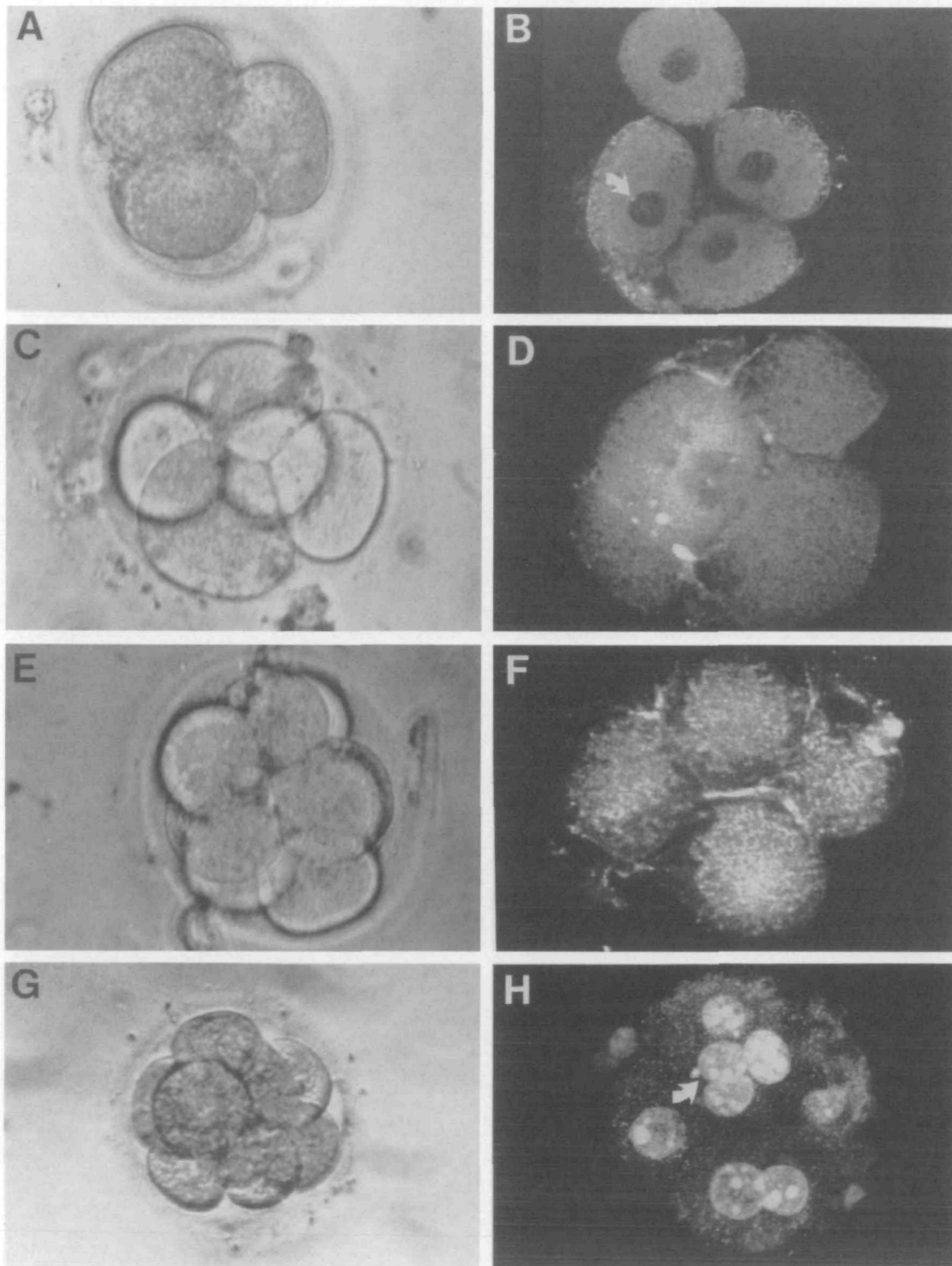


Figure 2. Phase contrast (left) and confocal (right) images of normally fertilized human embryos between the 4-cell and 8-cell stages. (A) 4-cell on day 2; (B) Confocal optical section through A showing one perinuclear spot of connexin 43 (Cx43); (C) 5-cell on day 2; (D) Confocal image of C showing trafficking of connexin 43 (Cx43) protein and insertion into the membrane; (E) 8-cell embryo on day 3; (F) Confocal image of E showing lining up of Cx43 in membrane; (G) 8-cell on day 4; (H) Confocal image of G showing absence of Cx43 labelling following incubation in phosphate-buffered saline (PBS) instead of primary anti-Cx43 antibody. Nuclei have been labelled with propidium iodide. Note binucleate cell (arrowed).

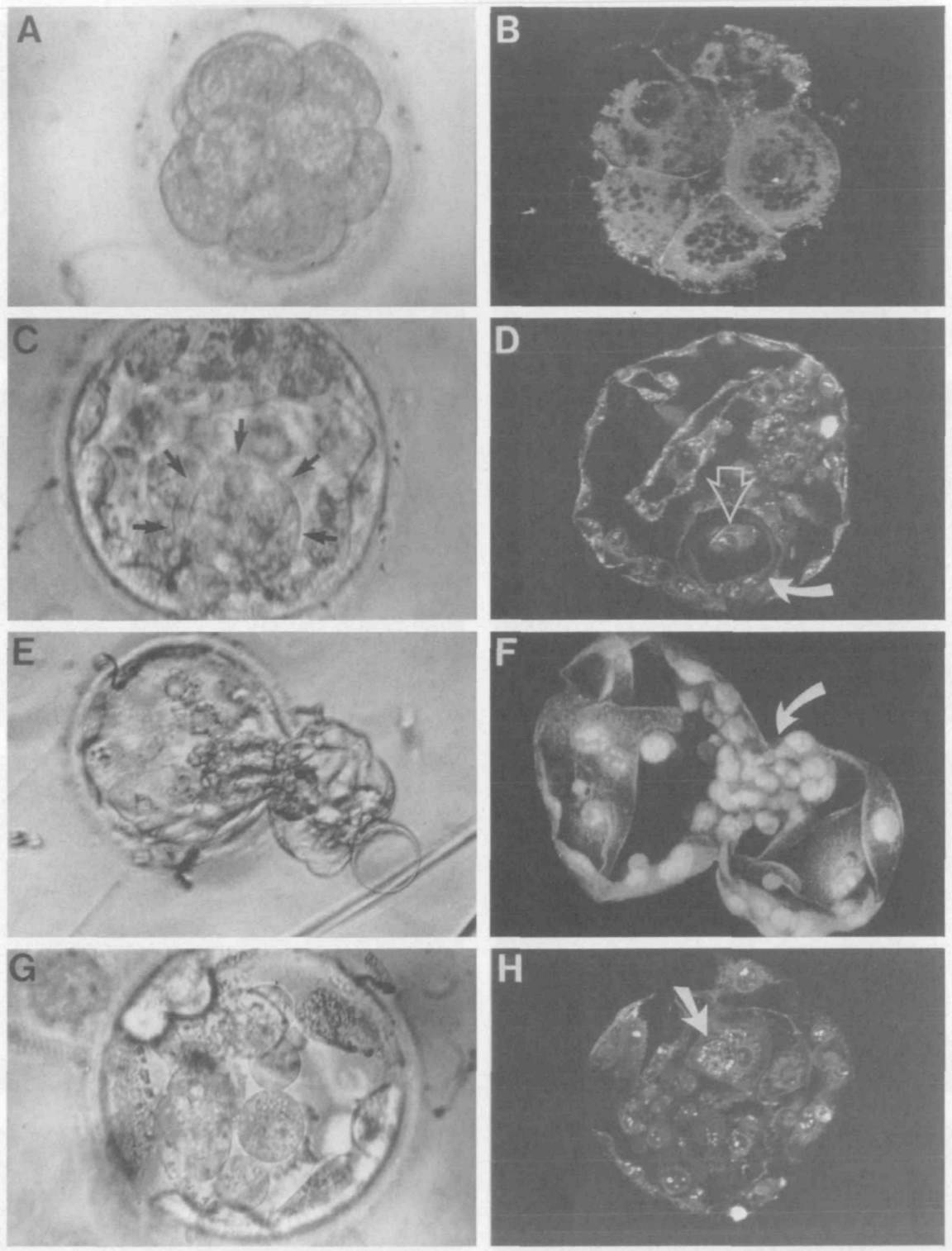


Figure 3. Phase contrast (left) and confocal (right) images of normally fertilized human embryos between the 10-cell and blastocyst stages. (A) 10-cell on day 3; (B) Confocal image of A showing lining up of connexin 43 (Cx43)-containing gap junction plaques between cells; (C) Blastocyst on day 5. Note vesicle in blastocoel cavity (arrowed); (D) Confocal optical section through C showing Cx43 staining and detail of a vesicle with the appearance of a smaller blastocyst complete with TE (solid arrow) and ICM (open arrow); (E) Hatching blastocyst on day 6; (F) Confocal image of E with nuclei labelled with propidium iodide. Note ICM at constriction (arrowed); (G) Blastocyst on day 5; (H) Confocal image of G showing Cx43 staining and an engulfed cell (arrowed).

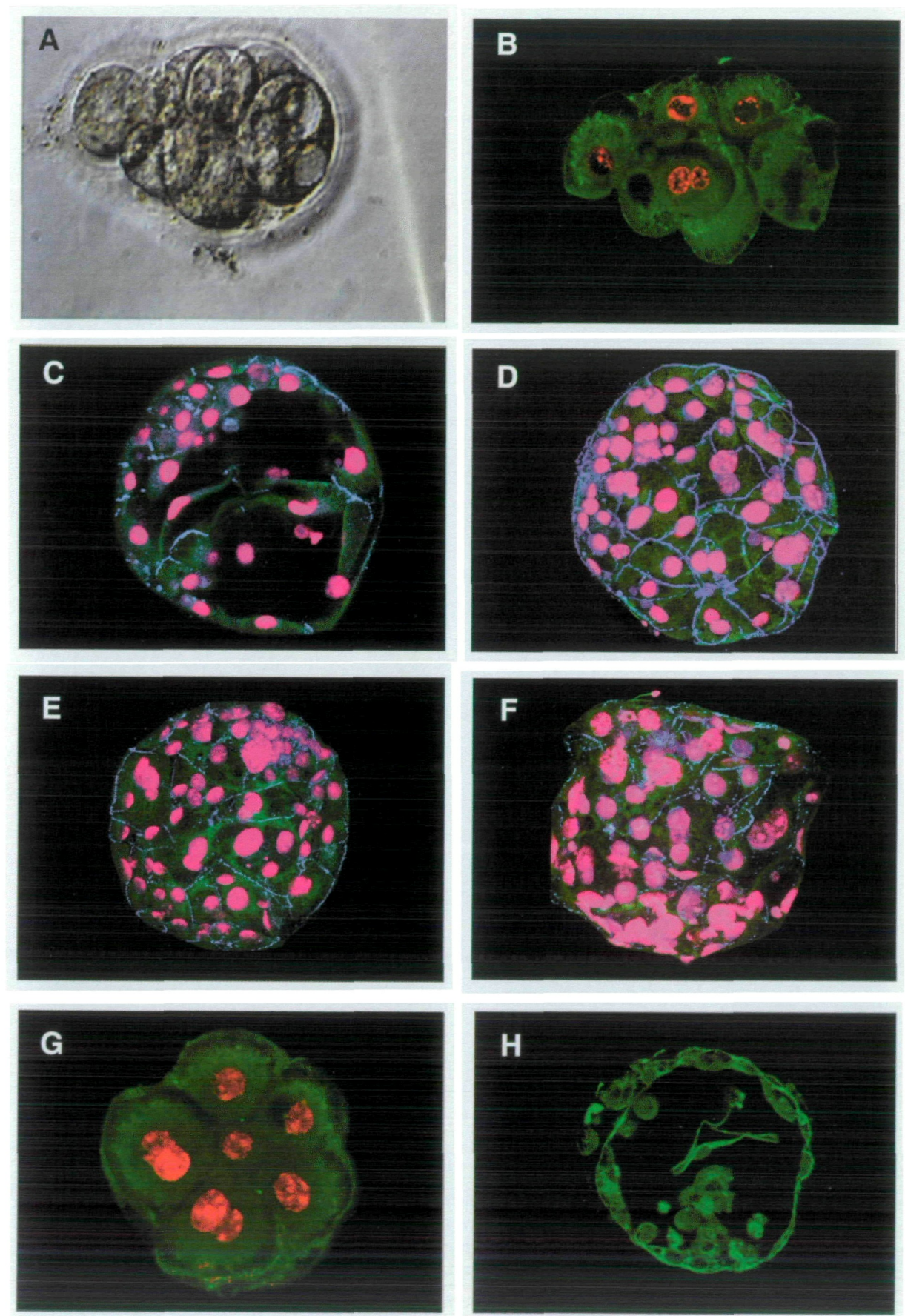


Figure 4.

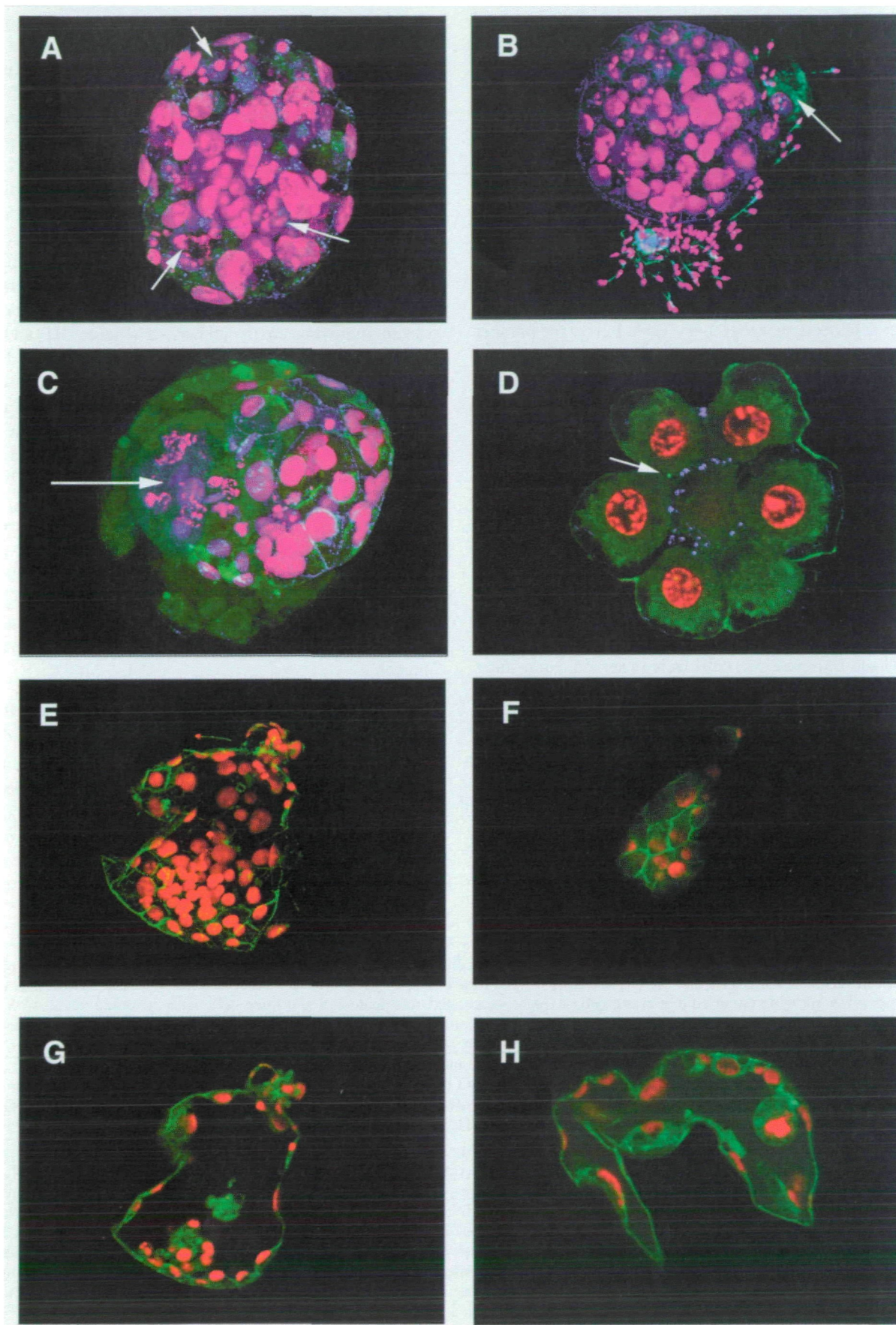


Figure 5.

iodide (Sigma) to label nuclei. Embryos were individually mounted on a slide in citifluor (City University) within a ring of clear nail varnish (three coats thick), a coverslip applied and sealed with nail varnish. For negative controls primary antibody was omitted.

Stained embryos were examined using multichannel confocal microscopy (Leica TCS 4D laser confocal microscope). Single confocal sections and projections through the embryo were collected, analysed for the distribution of gap junctions and desmosomes and photographed from the monitor.

Results

A total of 74 embryos, of which 62 were normally fertilized and 12 were abnormally fertilized, were donated by 25 patients (average three per patient, range 1–9). Table I gives the number of embryos examined between the 4-cell stage (day 2 after insemination) and the expanded blastocyst stage (days 5–7 after insemination). Of the 47 cleavage stage embryos (defined here as embryos up to and including the 16-cell stage) examined, 45 were of good quality (grade 1 or 2) on day 2, with all blastomeres intact and little or no fragmentation.

Development of the human preimplantation embryo in vitro

Figure 1 shows bright field photographs of living, normally fertilized human embryos during progression from the 4-cell stage to the expanded blastocyst. Figure 1A shows a normal 4-cell embryo 2 days after insemination. Embryos with 5 (Figure 1B) and 6 (Figure 1C) cells were observed, confirming that the early cleavages are asynchronous. Three days after insemination, most embryos were at the 8-cell stage (Figure 1D). During these early stages, the cells were usually round and only loosely apposed (e.g. Figure 1A,B,C). However, embryos with some cells that were partially flattened against each other were observed both at the 4-cell and 8-cell stages (Figure 1D). The transition from the 8- to 16-cells also was marked by asynchronous cleavage and 9-cell, 10-cell, 12-cell and 14-cell embryos were common (Figure 1E). Even at the

12- and 14-cell stages, the cells were clearly discernible, with little obvious signs of compaction (Figure 1E). Most 8- to 16-cell embryos possessed some cells which were closely apposed (Figure 1F), although there were no examples of embryos where all cells showed the close apposition and intercellular flattening that characterizes compaction in the mouse.

The transition between non-compacted, non-cavitating embryos and early blastocysts was rapid. Morula stage embryos, with 16 or more cells, were found only infrequently and did not show features characteristic of fully compacted embryos (Figure 1G). At cavitation, in contrast to the mouse, inner cell mass (ICM) cells remained round and loosely apposed (Figure 1H). ICM cells remained large and loosely packed following cavity expansion (Figure 1I), and did not form a discrete clump of cells as found in the mouse. However, as in the mouse, the trophoctoderm (TE) formed a single outer layer of tightly apposed cells. Condensation of ICM cells was not apparent until day 6 and 7, by which time the ICM in many late blastocysts had compacted to form a discrete collection of tightly packed cells at one pole of the blastocyst (Figure 1J).

Abnormalities that are not seen during normal mouse preimplantation development were common in human embryos. Vacuolated cells (Figure 1K) were observed in eight cleavage stage embryos (seven of which had been normally fertilized). Various degrees of cytoplasmic fragmentation were also common (Figure 1L), even during superficially normal development.

The pattern of intercellular junctions during preimplantation development

The distribution of gap junctions was analysed in these 74 embryos from the 4-cell stage through to the expanded blastocyst stage. Embryos were stained with anti-peptide or monoclonal antibodies specific for the gap junction connexin proteins Cx43, Cx32 and Cx26 (see Becker *et al.*, 1995 for antibody characterization) (Table I). The pattern is first described in

Figure 4. Confocal images of normally fertilized embryos at the 10-cell, 14-cell and blastocyst stage. Nuclei are labelled with propidium iodide, except in (H), and are red (B and G) or pink (C–F). (A) Phase contrast image of day 4 embryo with ~10 cells. (B) Single section confocal image of A showing engulfed binucleate cell, a single vacuolated, anucleate cell and three cells with apoptotic nuclei with marginalized chromatin. Very little connexin 43 (Cx43) labelling (green) is apparent. (C) Optical section through a blastocyst on day 6 showing punctate labelling of Cx43 (blue) between inner cell mass (ICM) cells. (D) Blastocyst on day 6 showing linear arrays of Cx43 labelling (blue) between TE cells. (E) Blastocyst on day 6 showing punctate labelling of Cx43 (blue) between trophoctoderm (TE) and ICM cells. (F) Expanded blastocyst on day 7 showing linear arrays of Cx43 (blue) between TE cells. However, this blastocyst was lacking an ICM. (G) Optical section through a day 4 embryo at 14-cell stage showing two binucleate cells and two desmosomal plaques (green). (H) Optical section of blastocyst on day 6 showing punctate labelling of Cx32 (green) between TE cells.

Figure 5. Confocal images of normally fertilized human embryos at the blastocyst and 14-cell stages. Nuclei are labelled with propidium iodide and are pink (A–C) or red (D–H). (A) Re-expanding blastocyst on day 7 following collapse 5 h previously. Note patches of apoptotic nuclei in the trophoctoderm (TE) (arrowed) and less organized labelling of connexin 43 (Cx43, blue) compared with those in Figure 4. (B) Collapsed blastocyst on day 6 with less organized labelling of Cx43 (blue). Note tuft of spermatozoa and excluded blastomere (arrowed) with no Cx43 labelling. (C) Blastocyst on day 7. On the left (arrowed) is a single 2-cell stage blastomere which has arrested, with four apoptotic nuclei. On the right is a morphologically normal 'mini' blastocyst with ~20 cells, and linear arrays of Cx43 labelling (blue) between the TE cells. The blastocyst also has an inner cell mass (ICM). Excluded anuclear fragments show no Cx43 labelling. (D) Optical section of day 4 14-cell embryo showing Cx43 labelling (blue) at inner basal cell–cell appositions and desmoplakin labelling (green, arrowed). (E) Serial reconstruction of the centre of an expanded, herniating, blastocyst on day 5 labelled with antibodies to desmoplakin (DPI21) (green). (F) Detail of the TE surface of expanded blastocyst in E showing linear arrays of desmoplakin labelling (green) between TE cells. (G) Single optical section through expanded blastocyst shown in E showing absence of desmoplakin labelling (green) in ICM. (H) Single optical section through expanded blastocyst on day 5 showing TE cell undergoing mitosis. The dividing cell is projecting into the blastocoel cavity and the desmosomes (green) have been marginalized to one pole of the cell.

cleaving embryos that had been normally fertilized, and which would, if returned to the uterus, be expected to have a good chance of implanting.

Gap junctions in normally fertilized embryos with good morphology

At the 4-cell stage ($n = 4$) Cx43 staining was apparent. All four embryos had cytoplasmic labelling in the perinuclear region (Figure 2A,B). Three also had occasional punctate Cx43 stain in apposing cell membranes. Three normal 5-cell embryos and four 6-cell embryos showed a similar pattern of punctate Cx43 label in apposed cell membranes, perinuclear labelling, and cytoplasmic Cx43 close to the membrane (Figure 2C,D).

By the 8-cell stage ($n = 6$) clear punctate, Cx43 staining was observed consistently in apposing cell membranes and in the cytoplasm. In regions where cellular apposition was weak, cytoplasmic Cx43 staining predominated. However, where cells were flattening against each other, the density of Cx43 labelling increased to give dense arrays of label in apposing membranes (Figure 2E,F). Similar 8-cell embryos incubated in the absence of primary antibodies were not labelled (Figure 2G,H). Of the embryos undergoing the fourth cleavage division (containing between 9 and 14 cells), 13 showed a similar pattern, with densely packed arrays of membrane Cx43 staining in regions of close cellular apposition (Figure 3A,B).

Of particular interest in relation to the selection of embryos for IVF was the morphologically normal embryo illustrated in Figure 4A,B. Despite its reasonably good morphology, this 10-cell embryo had very low levels of gap junction staining. Furthermore, the majority of cells were highly abnormal, with two vacuolated anucleate cells; two cells with marginalized chromatin in the nuclei, which is characteristic of nuclei undergoing apoptosis; and two binucleate cells. All other normal embryos at this stage showed clear evidence of gap junctions at membrane appositions.

Thus membrane-associated connexin 43 staining was observed as early as the 4-cell stage, when the cells were only loosely apposed. As the embryos matured from the 4-cell stage to the 16-cell stage, any increase in cellular apposition was paralleled by increased density of gap junctions in the membranes. Although human embryos do not become obviously compacted prior to cavitation, in contrast to mouse embryos, this does not prevent gap junction assembly.

A total of 11 expanding and expanded blastocysts between days 5 and 7 post-insemination showed extensive Cx43 staining, both between ICM cells (Figure 4C) and between TE cells (Figure 4D). Inner cells displayed intermittent punctate staining on apposed cell membranes (Figure 4C). In TE cells, a linear array of tightly packed gap junctions was apparent at the outermost edges, giving a 'pavement' appearance to the outermost cells (Figure 4D). Cytoplasmic labelling was observed, but it was neither as prominent nor as frequent as observed during early stages. Cx43 containing gap junctions were apparent between ICM and TE cells (Figure 4E) and were maintained between dividing cells.

One expanded blastocyst with apparently normal overall morphology showed an interesting and unexpected feature. Bright field examination suggested the presence of a large

vesicle within the blastocoel cavity (Figure 3C). After staining and observation in the confocal microscope, it was revealed as a small, but nevertheless complete, blastocyst (Figure 3D). Individual cells were clear and the mini blastocyst showed exactly the same gap junction staining pattern as the 'host' blastocyst. Figure 4F shows a day 7 expanded blastocyst, which displayed excellent morphology in the light microscope. However, after staining, confocal microscopy revealed that the ICM was non-existent and consisted only of one or two dead and dying cells. Figure 3E shows a hatching blastocyst that looks constricted through the ICM under the light microscope. After staining and confocal microscopy (Figure 3F) the embryo appeared to be in the process of separation into two, small blastocysts and could be twinning.

Many normally fertilized embryos of good morphology had one or more cells with nuclear abnormalities, as revealed by propidium iodide labelling. These included anucleate cells, binucleate cells and multinucleate cells (see for example, Figures 2H, 4B and 4G). Four out of 13 normally fertilized embryos (31%) undergoing the fourth cleavage division had one or more binucleate cells. Binucleate cells and cells with fragmenting/apoptotic nuclei also were present in blastocysts. Gap junction expression between these cells and neighbours was variable, but some binucleate cells clearly expressed Cx43 containing gap junctions in their membranes (Figure 4G). We also observed an apoptotic cell being engulfed by a neighbouring cell in a day 5 blastocyst (Figure 3H), which suggests that cells of the blastocyst may be capable of eliminating a small number of dead and dying cells. Previously phagocytosis was not believed to occur until later in development when specific phagocytic cell types differentiate.

One day 5 and five day 6 blastocysts were stained for Cx32. Two showed a small number of Cx32-containing gap junctions between trophoctoderm cells (Figure 4H), the remainder (two of which were collapsed) were unlabelled. Four day 6 and three day 7 expanded blastocysts were stained for Cx26. Only one day 6 blastocyst showed some staining between TE cells.

Gap junctions in normally fertilized, but morphologically abnormal embryos

Varying degrees of fragmentation were seen in 23 cleavage stage embryos. Cx43 containing gap junctions were not observed between cytoplasmic fragments.

Four collapsed blastocysts labelled with anti-Cx43 antibodies were examined. In two (day 5) there were a few disorganized Cx43 containing gap junctions. A third, collapsed day 7 blastocyst re-expanded over 5 h, and then was processed for immunocytochemistry (Figure 5A). Cx43-containing gap junction expression between TE cells was disorganized and reduced. In two areas of the TE, a number of neighbouring TE nuclei were fragmented, indicative of cell death and possible damage to the TE epithelium. In the fourth collapsed blastocyst (day 6), there were still some linear arrays of Cx43-containing gap junctions between TE cells (Figure 5B), although these showed less organization than in expanded blastocysts (compare Figure 4D). This blastocyst also had a larger excluded cell with little Cx43 expression.

A small, morphologically poor, day 7 blastocyst (Figure

5C) proved to have a large arrested blastomere, approximately at the 2-cell stage judging from the size, which had been excluded from the blastocyst and contained four fragmented nuclei. Before fixation, this cell had been pushed to the periphery of the embryo, surrounding a blastocyst of ~20 cells with both ICM and TE cells. There were also cytoplasmic fragments with no Cx43 containing gap junctions between them. It appears that at the 2-cell stage, one blastomere had arrested, although nuclear division continued, while the other blastomere continued normal development to the blastocyst stage. Whether this embryo would have the potential to implant is unknown. Arrest of an early cleavage stage blastomere with normal blastocyst formation in the remainder of the embryo has been observed in the baboon (Enders *et al.*, 1990).

A number of attempts were made to demonstrate the appearance of tight junctions using antibodies to the ZO-1 tight junction associated protein (kindly given to us by Bruce Stevenson). The ZO-1 antibodies did not stain the embryos and we have since found that these antibodies do not label tight junctions in adult human tissues and cell lines (Kurt Herrenknecht, personal communication). Presumably the epitope(s) of the available antibodies, although they show widespread cross-reactivity between non-human vertebrates, do not recognize the human ZO-1 protein.

Desmosomes in normal embryos

The opportunity was taken to examine the pattern of desmosome staining with antibodies to desmoplakin, which is expressed in all desmosomes. These embryos were routinely stained also with propidium iodide to reveal nuclear morphology. In embryos dividing to the 16-cell stage, single desmosomes were observed in an optical section, implying that final assembly of desmosomes was just underway (Figure 5D). In cavitating embryos desmosome assembly proceeded rapidly towards an extensive linear array between all TE cells (Figure 5E,F). Desmosomes were not observed in the ICM (Figure 5E,G), as noted for the mouse embryo (Fleming *et al.*, 1991). A trophoblast cell undergoing cell division in one day 5 blastocyst (Figure 5H) had rounded up into the blastocoel cavity, but maintained desmosome contacts with adjacent TE cells at one pole of the dividing cell. Thus neither gap junctions nor desmosomes disappear during cell division.

Intercellular junctions in abnormally fertilized and arrested embryos

Six embryos that had been abnormally fertilized and were polyspermic, together with 6 embryos where no evidence of fertilization had been seen on day 1, although they subsequently cleaved and may be parthenogenetic, were examined between the 4- and 8-cell stages. Some cells were multinucleate, as in normally fertilized embryos, but generally these embryos were of normal morphology. Cx43 containing perinuclear labelling and some punctate labelling in membranes was observed.

Six arrested embryos (four normally fertilized, two polyspermic) were examined between the 4- and 8-cell stages. All the normally fertilized embryos showed some perinuclear Cx43 and some spots of label in the membrane; however, there were no dense arrays of gap junctions.

Discussion

Gap junctions can be found in apposing cell membranes of the human embryo as early as the 4-cell stage. These gap junctions were detected with an antipeptide antibody for connexin 43 (Cx43). The epitope for this antibody has been identified as within the region EIKKFK in the cytoplasmic loop of mouse Cx43, which is completely conserved in the human homologue. Cx43 protein expression increased throughout preimplantation development, with dense arrays of gap junctions between trophoblast cells at the blastocyst stage, while ICM cells were linked by less frequent, punctate gap junctions. Gap junction plaques were observed between the two lineages, suggesting that they have the potential to communicate with each other. There was no substantial evidence to suggest that either Cx32 or Cx26 proteins were expressed prior to the late blastocyst stage. We conclude that early human embryos, like preimplantation mouse embryos (Nishi *et al.*, 1991; Becker *et al.*, 1992; 1995), express predominantly Cx43 protein in their gap junctions prior to implantation. In ultrastructural studies with human embryos, gap junctions were first observed at the 8-cell (Tesarik, 1989) and were found at morula stages (Dale *et al.*, 1991; Gualtieri *et al.*, 1992). More extensive gap junction expression was found in both the trophoblast (TE) and the inner cell mass (ICM) of human blastocysts (Lopata *et al.*, 1982; Mohr and Trounson, 1982; Lindenberg and Hyttel, 1989; Sathananthan *et al.*, 1990; Dale *et al.*, 1991; Gualtieri *et al.*, 1992).

The other features of Cx43 expression described here parallel observations in the mouse (reviewed Becker and Davies 1995). In human embryos of good morphology, Cx43 protein initially accumulates in the cytoplasm at the 4-cell stage, with occasional membrane insertion. In mouse embryos a similar cytoplasmic accumulation of connexin protein is seen at the 4–8-cell stage but in mice, the connexins are not inserted into the cell membranes until the compacting 8-cell stage (Becker *et al.*, 1992; De Souza *et al.*, 1993). During further cleavage, cytoplasmic label decreases as gap junctions continue to be inserted into the membrane. The density of gap junctions rises, particularly at the outermost apical edges of apposing cells, where gap junctions form a dense array. Unlike the mouse, there is little evidence of compaction in the human embryo until the 16-cell stage, and even then compaction is not complete. Our observations suggest that in the human embryo full compaction does not occur before the 16- to 32-cell stage, and that cavitation and blastocoel expansion is then initiated immediately. The timing of compaction varies between mammalian species, ranging from the 8-cell stage in the mouse, the 16- to 32-cell stage in bovine embryos, through the 32- to 64-cell stage in rabbit embryos (Koyama *et al.*, 1994), to just before blastocyst formation with pig embryos (Reima *et al.*, 1993). Variable degrees of compaction have been observed in embryos of non-human primate species, such as the baboon (Panigel *et al.*, 1975) and the rhesus monkey (Hurst *et al.*, 1978; Enders and Schlafke, 1981) where uncompacted embryos with 20 or more cells have been observed.

The appearance of tight junctions, which seal the developing intercellular cavities from the extra-embryonic environment,

is a necessary pre-requisite to the establishment of the two early lineages, the ICM and the TE. In the mouse this occurs at compaction during the 8-cell stage, before blastocoel expansion begins, and the subsequent cleavage to 16-cells generates inner and outer cells with separate lineages. In human blastocysts, extensive tight junctions that exclude lanthanum from the blastocoel cavity (Gualtieri *et al.*, 1992) have been observed by TEM at apical points between mural TE cells (Lopata *et al.*, 1982; Mohr and Trounson, 1982; Lindenberg and Hyttel, 1989; Sathananthan *et al.*, 1990). Although available antibodies to the tight junction associated protein ZO-1 apparently do not cross-react with human tissues, ultrastructural studies suggest relatively early assembly of tight junctions in human embryos. Focal contacts that might be tight junctions have been observed ultrastructurally from the 6-cell (Dale *et al.*, 1991) or 8-cell stages (Tesarik, 1989). However, serial sectioning at the 6- to 10-cell stage (Dale *et al.*, 1991) and lanthanum tracing combined with TEM at the morula stage (Gualtieri *et al.*, 1992) suggested that these junctions are not yet zonular. Taken together, these results suggest that in the human embryo separation into TE and ICM lineages may not occur until the blastocyst stage.

Desmoplakin is characteristic of mature desmosomes and the first desmosomes were observed during cleavage to the 16-cell stage. In blastocysts, mature desmosomes were found between all trophectoderm cells, although not between cells of the ICM nor between ICM and TE cells, in agreement with immunocytochemical observations on mouse embryos by Fleming *et al.* (1991). Ultrastructural studies have described focal intercellular junctions which have been termed primitive desmosomes in 4-cell stage human embryos fertilized both *in vivo* (Pereda *et al.*, 1989) and *in vitro* (Trounson and Sathananthan, 1984; Sathananthan *et al.*, 1990; Dale *et al.*, 1991). Mature desmosomes have been extensively described at the ultrastructural level in human blastocysts (Lopata *et al.*, 1982; Mohr and Trounson, 1982; Lindenberg and Hyttel, 1989; Sathananthan *et al.*, 1990) although Gualtieri *et al.* (1992) did not observe them using TEM at morula and blastocyst stages. The presence of a variety of cell adhesion molecules on the preimplantation human embryo has been described (Campbell *et al.*, 1995) but their precise relation to gap junction expression is not immediately clear.

In the mouse embryo, the presence of Cx43 staining gap junctions in apposing cell membranes is associated with efficient functional intercellular communication through gap junctions from the 8-cell stage onwards, as evidenced by the transfer of small fluorescent dyes, such as Lucifer Yellow (Lo and Gilula, 1979; Goodall and Johnson 1982; Lee *et al.*, 1987; Becker *et al.*, 1995), while large molecules such as the dextrans are excluded. Dale *et al.* (1991) reported a failure of cell-to-cell transfer of Lucifer Yellow in human embryos prior to the blastocyst stage. This is surprising, considering the immunocytochemical and ultrastructural evidence of gap junctions from the 4-cell stage onwards. Dale *et al.* (1991) did not test for the presence of ionic communication or other small dyes that might be expected to transfer through gap junctions. It is possible that gap junctions remain in a non-functional state in human embryos until the blastocyst stage, which raises the

interesting question of how such repression of functional communication might be regulated. However, the sample examined by Dale *et al.* (1991) was relatively small (13 embryos in total) compared with the sample examined here (74 embryos) and it is possible that the few embryos examined by them prior to the blastocyst stage were indeed non-communicating. We are now trying to resolve this issue.

We have examined a large number of human embryos from the 4-cell stage on day 2 after insemination to the expanded and hatching blastocyst stage on day 7. Although the majority of embryos were described as being of good morphology on day 2 (grades 1 and 2), the cellular morphology was variable as development progressed. Anucleate fragments and decompacted and excluded blastomeres were observed frequently, with these embryos showing poor gap junction expression. The blastocysts observed in this study exhibited a variable morphology, with many interesting features. One expanded day 5 blastocyst contained a smaller vesicle of cells which closely resembled a small but perfectly formed blastocyst (Figure 3D). The developmental potential of this is unknown, but could provide a possible mechanism for twin formation. Two possible mechanisms of twin formation (suggested by Edwards *et al.*, 1986; Cohen *et al.*, 1990) were demonstrated in a day 6 hatching blastocyst, where the ICM had been divided by the constriction caused by the zona pellucida at the site of hatching (Figure 3E,F). If the hatched portion was 'nipped' off before the embryo was able to complete the hatching process, this would result in two blastocysts, each with an ICM (dichorionic identical twins). Alternatively, if the ICM became divided into two clumps, within one blastocyst, monochorionic identical twins would result. Blastocysts which expanded, but subsequently collapsed, appeared to be compromised. One day 7 blastocyst showed regions of dying TE (Figure 5A) and in other collapsed blastocysts gap junction expression became disorganized. Finally, a day 7 expanded blastocyst which looked morphologically healthy, was shown on closer examination by confocal microscopy to lack a healthy ICM (Figure 4F). This blastocyst would probably have the potential to implant, and produce chorionic gonadotrophin, but would be unable to develop further, giving rise to a biochemical pregnancy following embryo transfer.

Many normally fertilized human preimplantation embryos, including those of good morphology which would be considered for transfer, were revealed by confocal microscopy to be compromised, indicating that normal morphology in the light microscope is not necessarily a good guide to embryo quality. Apparently superficially normal cleavage stage embryos were found to lack Cx43 containing gap junctions. Nuclear labelling revealed a high incidence of cellular and nuclear abnormalities. The detection of binucleate and anucleate blastomeres, as well as apoptotic cells with nuclei with marginalized chromatin or undergoing fragmentation, confirms previous observations in human embryos (Hardy *et al.*, 1989; 1993; Hardy, 1993). A limited number of dying cells may be eliminated by phagocytosis, but widespread nuclear abnormalities would be expected to compromise normal development. Cells with abnormal nuclei generally exhibited poor Cx43 containing gap junction

expression, suggesting that only healthy cells are capable of communication.

Our results suggest that when patients have a consistent record of failure of apparently viable embryos to implant, it would be worth more detailed morphological examination to eliminate a contribution from the abnormalities revealed here by confocal microscopy. Progressively decompacting cells which subsequently die and have poor gap junctional communication are a feature of mouse embryos with the DDK syndrome (Buehr *et al.*, 1987); 90% of these embryos die before implantation. These embryos can be temporarily rescued by modifications of the environment that improve junctional communication and organization, such as increasing intracellular pH or cAMP levels (LeClerc *et al.*, 1994). One of the causes of embryonic arrest in the human preimplantation embryo is suboptimal culture conditions, and it will be interesting to see whether modifying the culture medium can improve gap junction organization and cell-cell communication and hence blastocyst formation and ultimate survival.

Acknowledgements

We thank Kate Whitley for help in preparing the figures, Bruce Stevenson for the gift of ZO1 antibodies, Anthony McGee for the DP121 antibody. D.L.B. and A.E.W. thank the Royal Society for their support. This work would not have been possible without earlier support from the Wellcome Trust (Grant numbers: 35019/91/MJM; 03220/2/1.5) during which the anti-connexin antibodies were generated and characterized.

References

Becker, D.L. (1996) Value of confocal microscope digital imaging and reconstruction using RGB colour technology. *Hum. Reprod. Update*, **2** (in press).

Becker, D.L. and Davies, C.S. (1995) The role of gap junctions in the development of the preimplantation mouse embryo. In Gourdie, R. (ed.), *Microscopy of Intercellular Communication Junctions*. Vol. 31. pp. 364–374.

Becker, D.L., David-Leclerc, C. and Warner, A.E. (1992) The relationship of gap junctions and compaction in the preimplantation mouse embryo. *Development*, (Suppl), 113–118.

Becker, D.L., Evans, W.H., Green, C.R. and Warner, A.E. (1995) Functional analysis of amino acid sequences in connexin 43 involved in intercellular communication through gap junctions. *J. Cell Sci.*, **108**, 1455–1467.

Bevilacqua, A., Loch-Carusio, R. and Erickson, R.P. (1989) Abnormal development and dye coupling produced by antisense RNA to gap junction protein in mouse preimplantation development. *Proc. Natl. Acad. Sci. USA*, **86**, 5444–5448.

Buehr, M., Lee, S., McLaren, A. and Warner, A. (1987) Reduced gap junctional communication is associated with the lethal condition characteristic of DDK mouse eggs fertilized by foreign sperm. *Development*, **101**, 449–459.

Campbell, S., Swann, H.R., Seif, M.W. *et al.* (1995) Cell adhesion molecules on the oocyte and preimplantation human embryo. *Mol. Hum. Reprod.*, **1**, see *Hum. Reprod.*, **10**, 1571–1578.

Cohen, J., Elsner, C., Kort, H. *et al.* (1990) Impairment of the hatching process following IVF in the human and improvement of the implantation by assisting hatching using micromanipulation. *Hum. Reprod.*, **5**, 7–13.

Dawson, K.J., Conaghan, J., Ostera, G.R. *et al.* (1995) Delaying transfer to the third day post-insemination, to select non-arrested embryos, increases development to the fetal heart stage. *Hum. Reprod.*, **10**, 177–182.

Dale, B., Gualtieri, R., Talevi, R. *et al.* (1991) Intercellular communication in the early human embryo. *Mol. Reprod. Dev.*, **29**, 22–28.

De Souza, P., Valdimarson, G., Nicholson, B.J. and Kidder, G.M. (1993) Connexin trafficking and the control of gap junction assembly in preimplantation mouse embryos. *Development*, **117**, 1355–1367.

Ducibella, T., Albertini, D.F., Anderson, E. and Biggers, J.D. (1975) The preimplantation mammalian embryo; characterization of intercellular junctions and their appearance during development. *Dev. Biol.*, **45**, 231–250.

Edwards, R.G., Mettler, L.E. and Walters, D.E. (1986) Identical twins and in-vitro fertilization. *J. In Vitro Fertil. Embryo Transfer*, **3**, 114–117.

Enders, A.C. and Schlafke, S. (1981) Differentiation of the blastocyst of the rhesus monkey. *Am. J. Anat.*, **162**, 1–21.

Enders, A.C., Lantz, K.C. and Schlafke, S. (1990) The morula-blastocyst transition in two old world primates: the baboon and rhesus monkey. *J. Med. Primatol.*, **19**, 725–747.

Fleming, T.P., Garrod, D.R. and Elsmore, A.J. (1991) Desmosome biogenesis in the mouse preimplantation embryo. *Development*, **112**, 527–539.

Goodall, H. and Johnson, M.H. (1982) Use of carboxyfluorescein diacetate to study formation of permeable channels between mouse blastomeres. *Nature*, **295**, 524–526.

Gualtieri, R., Santella, L. and Dale, B. (1992) Tight junctions and cavitation in the human pre-embryo. *Mol. Reprod. Dev.*, **32**, 81–87.

Hardy, K. (1993) Development of human blastocysts *in vitro*. In Bavister, B.D. (ed.), *Preimplantation Embryo Development*. Springer-Verlag, New York. pp. 184–199.

Hardy, K., Handyside, A.H. and Winston, R.M.L. (1989) The human blastocyst: cell number, death and allocation during late preimplantation development *in vitro*. *Development*, **107**, 597–604.

Hardy, K., Winston, R.M.L. and Handyside, A.H. (1993) Binucleate blastomeres in normally fertilized preimplantation human embryos *in vitro*: failure of cytokinesis during early cleavage. *J. Reprod. Fertil.*, **98**, 549–558.

Human Fertilisation and Embryology Authority (1994) *Annual Report*. HFEA, London.

Hurst, P.R., Jefferies, K., Eckstein, P. and Wheeler, A.G. (1978) An ultrastructural study of preimplantation uterine embryos of the rhesus monkey. *J. Anat.*, **126**, 209–220.

Koyama, H., Suzuki, H., Yang, X. *et al.* (1994) Analysis of polarity of bovine and rabbit embryos by scanning electron microscopy. *Biol. Reprod.*, **50**, 163–170.

LeClerc, C., Becker, D.L., Buehr, M. and Warner, A.E. (1994) Low intracellular pH is involved in the early embryonic death of a DDK mouse fertilized by alien sperm. *Dev. Dynam.*, **200**, 257–267.

Lee, S., Gilula, N.B. and Warner, A.E. (1987) Gap junctional communication and compaction during preimplantation stages of mouse development. *Cell*, **51**, 851–860.

Lindenberg, S. and Hyttel, P. (1989) *In vitro* studies of the peri-implantation phase of human embryos. In Van Blerkom, J. and Motta, P.M. (eds), *Ultrastructure of Human Gametogenesis and Early Embryogenesis*. Kluwer Academic Publishers, Boston. pp. 201–211.

Lo, C.W. and Gilula, N.B. (1979) Gap junctional communication in the preimplantation mouse embryo. *Cell*, **18**, 399–409.

Lopata, A., Kohlman, D.J. and Kellow, G.N. (1982) The fine structure of human blastocysts developed in culture. In *Embryonic Development, Part B: Cellular Aspects*. Alan R. Liss, New York, pp. 69–85.

Mohr, L.R. and Trounson, A.O. (1982) Comparative ultrastructure of hatched human, mouse and bovine blastocysts. *J. Reprod. Fertil.*, **66**, 499–504.

Nishi, M., Kumar, N.M. and Gilula, N.B. (1991) Developmental regulation of gap junction gene expression during mouse embryonic development. *Dev. Biol.*, **146**, 117–130.

Panigel, M., Kraemer, D.C., Kalter, S.S. *et al.* (1975) Ultrastructure of cleavage stages and preimplantation embryos of the baboon. *Anat. Embryol.*, **147**, 45–62.

Pereda, J., Cheviakoff, S. and Croxatto, H.B. (1989) Ultrastructure of a 4-cell human embryo developed *in vivo*. *Hum. Reprod.*, **4**, 680–688.

Reima, I., Lehtonen, E., Virtanen, I. and Flechon, J.E. (1993) The cytoskeleton and associated proteins during cleavage, compaction and blastocyst differentiation in the pig. *Differentiation*, **54**, 35–45.

Sathananthan, H., Bongso, A., Ng, S.-C. *et al.* (1990) Ultrastructure of preimplantation human embryos co-cultured with human ampullary cells. *Hum. Reprod.*, **5**, 309–318.

Tesarik, J. (1989) Involvement of oocyte-coded message in cell differentiation control of early human embryos. *Development*, **105**, 317–322.

Trounson, A. and Sathananthan, A.H. (1984) The application of electron microscopy in the evaluation of two- to four-cell human embryos cultured *in vitro* for embryo transfer. *J. In Vitro Fertil. Embryo Transfer*, **1**, 153–165.

Warner, A.E. (1992) Gap junctions in development—a perspective. *Semin. Cell Biol.*, **3**, 81–91.

Received on February 15, 1996; accepted on May 16, 1996